MINISTRY OF EDUCATION AND TRAINING
VIETNAM ACADEMY OF SCIENCE AND TECHNOLOGY

GRADUATE UNIVERSITY OF SCIENCE AND TECHNOLOGY

Nguyen Xuan Quang

SYNTHESIS AND CHARACTERIZATION OF Au – BASED NANOCOMPOSITE MATERIALS WITH CURCUMIN, ZINC OXIDE, AND SILVER FOR THE ENHANCEMENT OF KILLING PATHOGENS

SUMMARY OF DISSERTATION ON SCIENCES OF MATTER

Major: Materials for Electronics

Code: 9 44 01 23

Ha Noi – 2024

The dissertation is completed at: Graduate University of Science and Technology, Vietnam Academy Science and Technology

Supervisors:

1. Associate Prof. Dr. Tran Quang Huy
2. Prof. Dr. Vu Đinh Lam

Referee 1: Associate Prof. Dr. Le Tuan Tu
Referee 2: Associate Prof. Dr. Nguyen Xuan Ca
Referee 3: Associate Prof. Dr. Vu Duc Chinh

The dissertation is examined by Examination Board of Graduate University of Science and Technology, Vietnam Academy of Science and Technology at 14:00 September 28, 2024

The dissertation can be found at:

1. Graduate University of Science and Technology Library
2. National Library of Vietnam

INTRODUCTION

In recent decades, industrial and agricultural production in the world has developed dramatically. Along with that, environmental pollution is increasing, especially in developing countries like Vietnam. Environmental pollution seriously affects the quality of life and is one of the leading causes of communicable and non-communicable diseases globally. Vietnam is located in the Asia Pacific, which is one of the most heavily affected regions by communicable diseases. Normally, communicable diseases result in favorable conditions for the spread of opportunistic bacteria, thereby causing superinfection in patients. Furthermore, bacterial strains have become antibiotic-resistant or multidrug-resistant due to the uncontrolled use of antibiotics in medicine and agriculture. Therefore, patients infected with these strains of bacteria face many difficulties in treatment. Currently, a large number of hospitals have recognized the appearance of antibiotic-resistant or multidrug-resistant (MDR) bacterial strains such as the intestinal disease-causing bacteria *Escherichia coli* O157:H7 (*E. coli* O157:H7), methicillin-resistant *Staphylococcus aureus* (MRSA), vancomycin-resistant *Enterococcus* (VRE), multidrug-resistant *Mycobacterium tuberculosis* (MDR-TB), carbapenem-resistant *Enterobacteriaceae* (carbapenem-resistant *Enterobacteriaceae* - CRE), etc. Among them, many bacterial strains are resistant to even the latest generation of antibiotics. Treating infections caused by antibiotic-resistant bacteria is often complicated and expensive. In addition, treatment becomes harder if accompanied by communicable diseases or underlying medical conditions (e.g. Covid-19, AIDS). Many alternative solutions have been proposed, but their effectiveness depends largely on the disease condition. Furthermore, some solutions have posed potential side effects as well as long-term health risks and are life-threatening to patients. The World Health Organization (WHO)

has listed communicable diseases caused by antibiotic-resistant strains of bacteria as one of ten global life-threatening issues. Thus, it is urgent for scientists to look for suitable alternatives to current antibiotics in the fight against antibiotic-resistant bacterial strains. In the past two decades, nanotechnology has shown potential in solving this problem. At the nanoscale, materials exhibit unique properties that they do not have at the bulk size. Furthermore, at this scale, materials can easily circulate throughout the body to reach the target tissue or pathogenic bacteria infected inside organs of the body. Some types of inorganic nanomaterials have been studied and applied in biomedicine due to their special properties such as nano-magnetic (controlled by an external magnetic field, magnetothermal effect, etc.), nanosilver (antibacterial activity, photothermal effect, etc.), zinc oxide (antibacterial activity, anti-ultraviolet ray, etc.), titanium oxide (antibacterial activity, anti-ultraviolet rays, etc.), nano gold (drug-conducting, compatible biology, photothermal effect, etc.), titanium (implant material, biocompatibility, etc.). Recently, many studies on nanomaterial systems combining two metals, metal-metal oxide, and metal/metal oxide-drug molecules/active compounds from nature have also been studied to develop and exploit the advantages of each component material. One of the most popular nanomaterials in biomedical applications is gold nanoparticles (Au-NPs). Au-NPs possess superior properties such as surface plasmon effect, high biocompatibility, stable structure and easy surface functionalization to bind with other agents such as biological molecules, as well as drug molecules/active ingredients. Therefore, the combination of Au-NPs with inorganic elements or organic ingredients, are being furthered in biomedical applications. In reality, Au-NPs have been investigated to kill cancer cells, and carry drugs in targeted therapy, biological imaging, and in diagnosing pathogens and other biomedical applications. Recent studies also show that

the combination of Au-NPs with other substances such as drug molecules or natural active compounds (curcumin, berberin); active metals (Ag, Cu) or active metal oxides (ZnO, TiO_2) not only promotes the properties of Au-NPs but also contributes to enhancing effectiveness as well as biological activity of the combined elements. When a laser beam of appropriate wavelength is irradiated into Au-NPs, it will increase the local heat around them based on the photothermal effect. The local increase in heat of Au-NPs helps directly destroy pathogens or provide heat energy to stimulate the release of combined particles (drug molecules, active compounds, ions, etc.), indirectly contributing to the inhibition or destruction of pathogens without affecting surrounding healthy cells.

Therefore, studying the properties of the combination of Au-NPs with organic particles such as drugs/natural compounds (e.g. curcumin) or with inorganic materials with antibacterial properties (e.g. nano zinc oxides or Au-NPs) is a topic of great interest. In order to be applicable in biomedicine, nanocomposites must have high purity and not contain harmful residues that are toxic to living organisms. Besides, the availability of raw materials and active ingredients is also a matter of concern. However, the first challenge is to find a suitable manufacturing method under Vietnam's experimental settings to attain nanocomposite product which has high cleanliness and can be proactive in raw material sources. Secondly, it is required to analyze specific properties of this combination used in biomedical applications. The topic of the thesis is developed thanks to references from domestic and international articles recently published by the nBIORD lab. The electrochemical technology was developed to synthesize metallic nanoparticles from bulk materials. The study aims to synthesize gold-based nanocomposites with one of the known antibacterial agents

including the active compound from nature (curcumin) and inorganic elements (ZnO, Ag). Also, nanocomposites were studied to investigate the influence of Au-NPs on the properties and biological activities of the above agents to their ability to resist pathogenic bacteria causing hospital infections (including *E. coli* O157:H7 and *MRSA*) under circumstances of light exposure and non-exposure. In this study, blue laser light with a safe wavelength range (532 nm) was used to investigate the photothermal effect of gold-based nanocomposites aimed at treating skin infections such as burns or open wounds without affecting healthy tissues as well as the wound area where new skin is forming. For the above reasons, along with the lab's current equipment conditions and the mentorship of my supervisors, I decided to study the topic named "Synthesis and characterization of gold-based nanocomposite materials with curcumin, zinc oxide, and silver for the enhancement of killing pathogens" for my PhD thesis.

CHAPTER I: OVERVIEW

1.1. Characteristic properties of nanogold

Presentation of gold nanoparticles: properties (surface plasmon resonance effect, photothermal effect), fabrication methods and applications in the field of biomedical materials.

1.2. Gold - active ingredient from natural curcumin nanocomposite and applications

Presentation of curcumin, Au/Cur – CNPs: properties, fabrication methods and applications in the field of biomedical materials.

1.3. Gold - zinc oxide nanocomposite and applications

Presentation of ZnO - NPs, Au/ZnO – CNPs: properties, fabrication methods and applications in the field of biomedical materials.

1.4. Gold–silver nanocomposite and applications

Presentation of Ag – NPs, Au/Ag – CNPs: properties, fabrication methods and applications in the field of biomedical materials.

1.5. Analytical methods used in the thesis

Presenting methods and techniques for analyzing the characteristics of composite nanomaterial systems that have been reviewed and used in the thesis research.

CHAPTER 2. FABRICATION AND CHARACTERISTICS OF GOLD - CURCUMIN NANOCOMPOSITES

2.1. Materials and methods

2.1.1. Reagents

Gold bars (99.999%) with dimensions of 60 mm x 5 mm x 0.1 mm (length x width x thickness) were purchased from a jewellery store in Hanoi, Vietnam. Trisodium citrate ($Na_6H_5O_7$) was purchased from Sigma–Aldrich; curcumin was provided by the Institute of Chemistry, Vietnam Academy of Science and Technology. Two strains of bacteria causing nosocomial infections including *Escherichia coli* O157:H5 (*E.coli* O157:H7) and Methicillin-resistant *Staphylococcus aureus* (*MRSA*) were isolated and provided by the National Institute of Hygiene and Epidemiology, Vietnam. Other chemicals were of analytical grade.

2.1.2. Experimental method

a. Synthesis of gold-curcumin nanocomposites.

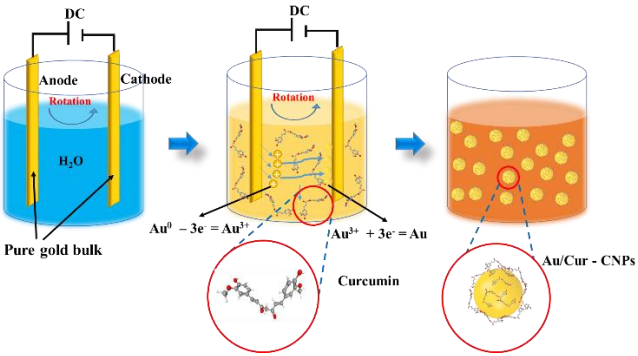

Figure 2.1. Synthesis of gold-curcumin nanocomposites by electrochemical method.

b. Analysis of the properties, antibacterial ability and cytotoxicity of the Au/Cur - CNPs

The formation and physicochemical properties of Au-NPs and Au/Cur - CNPs were investigated by UV-vis absorption spectroscopy (SP - 3000 nano, Optima); transmission electron microscopy (TEM, JEM1010, JEOL); X-ray diffraction (XRD, EQUINOX 5000, Thermo Scientific). Dynamic size and particle stability in solution were measured by dynamic light scattering (DLS), Zeta potential (Zetasizer Nano ZS) and near-IR absorption spectroscopy (FT-IR 4600). The photothermal measurement system was designed including a blue laser head with a wavelength of 532 nm and a thermal sensor that records temperature over time. The antibacterial activity and cytotoxicity of Au - NPs and Au/Cur - CNPs was evaluated through two bacterial strains causing hospital infections (including *E.coli* O157:H7 and *MRSA*) and MA – 104 cell line, respectively.

2.2. Results and discussion

2.2.1. Optical properties of Au – NPs and Au/Cur - CNPs.

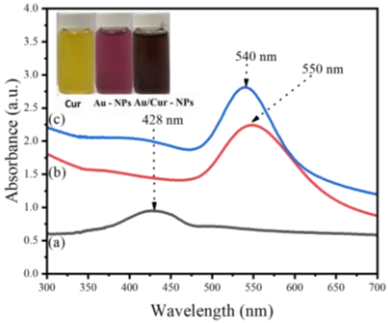

Figure 2.2. UV-Vis absorption spectrum of curcumin (a); Au - NPs (b); and Au/Cur - CNPs (c).

Au - NPs and Au/Cur - CNPs were prepared by the electrochemical method shows that the color of the solution without curcumin has changed from pink to bright red when observed with the naked eye. With the presence of curcumin during the electrochemical process, the solution has a plum-red color. Figure 2.2c is the UV - Vis absorption spectrum of the electrochemical solution containing curcumin molecules with two characteristic absorption peaks at wavelengths of 428 nm and 540 nm corresponding to curcumin and Au-NPs. Thus, it can be said that Au/Cur – CNPs were formed during the electrochemical process.

2.2.2. Morphology and structure of Au - NPs and Au/Cur – CNPs

Figure 2.3 shows TEM images of Au-NPs formed in the electrochemical solution without curcumin molecules with a spherical shape and an average particle size of 19.5 nm. For the sample added with curcumin, the majority of Au/Cur - CNPs were also formed in spherical shape, small size, with an average particle size of 13.6 nm, and surrounded by curcumin

molecules. The structure and crystal phase of Au/Cur - CNPs were investigated by X-ray diffraction (XRD).

The XRD pattern of the Au/Cur - CNPs also appears peaks characteristic of the face-centered cubic structure of gold, with Miller index (*hkl*) of (111); (200); (220) and (311), corresponding to diffraction angle positions of 37.38°; 43.52°; 63.94° and 77.22°. In addition to the characteristic diffraction peaks of Au - NPs, there are also peaks at angles of 27.75°; 39.93° and 49.72° are the diffraction peaks of curcumin. This result shows that, using the simple electrochemical method, it is possible to synthesize AuNPs/Cur -CNPs consisting of only two components Au and Cur with good crystallinity and high cleanliness.

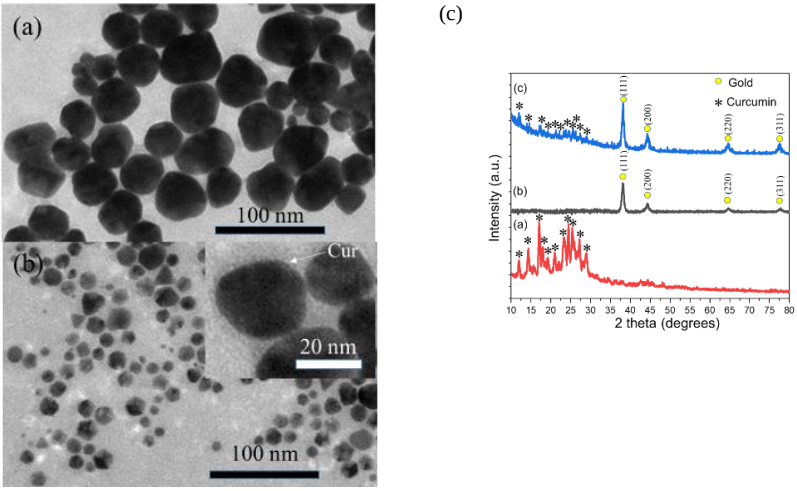

Figure 2.3. TEM images of (a) Au-NPs; (b) Au/Cur – CNPs; (c) X-ray diffraction patterns of curcumin, Au - NPs and Au/Cur – CNPs

2.2.3. Characterization of Au - NPs and Au/Cur - CNPs

a. FTIR absorption spectrum

FTIR spectrum analysis can clarify the connection between gold nanoparticles and curcumin molecules through changes in the vibrational mode of bonds existing on the surface of Au - NPs. From the FTIR absorption spectrum, it can be seen that the peaks specific to bonds of curcumin do not change much, and no new binding peaks appear. However, there is a shift in peak position. The obtained results once again confirm that Au/Cur – CNPs have been successfully synthesized by the electrochemical method.

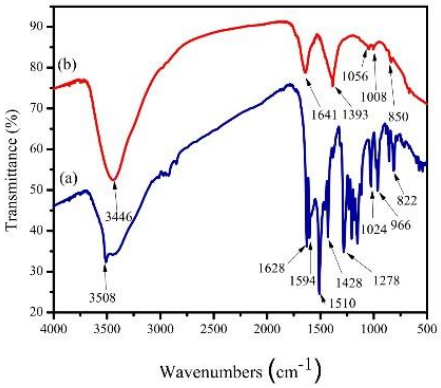

Figure 2.4. FTIR absorption spectrum of curcumin (a) and Au/Cur - CNPs (b).

a) Kinetic size and Zeta potential of Au/Cur – CNPs

The dispersibility and stability of Au/Cur - CNPs were evaluated through dynamic scattering (DLS) analysis and Zeta potential measurements. The results confirmed the role of curcumin molecules in reducing the size of gold nanoparticles and increasing the surface stability of Au - NPs.

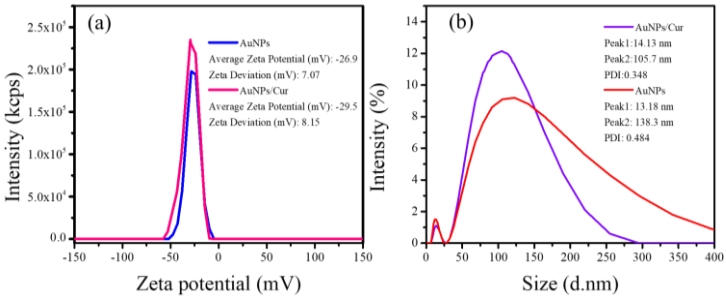

Figure 2.5. DLS (a) and Zeta potential (b) of Au - NPs and Au/Cur - CNPs

2.2.4. The photothermal effect of Au/Cur – CNPs

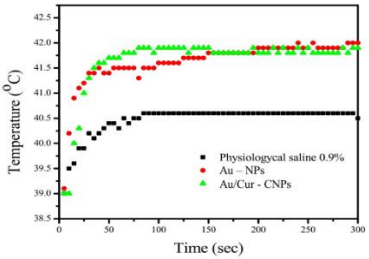

Figure 2.6. Increase of solution temperature with the time of 532 nm laser irradiation for 0.9% physiological saline, Au - NPs and Au/Cur – CNPs.

The photothermal effect was investigated based on the change in temperature of 0.9% physiological saline, Au – NPs, and Au/Cur - CNPs corresponding to the irradiation time with a 532 nm green laser source (Fig.2.6). Under steady-state conditions at 37°C, the temperature of all solutions increased and reached saturation after 90 sec of laser radiation. For physiological saline, the temperature increased by 1.5 °C. Meanwhile, the temperature in the tubes containing Au - NPs and Au/Cur - NPs increased by

an average of 3 ^{o}C. Thus, the curcumin shell does not affect the photothermal effect of Au.

2.2.5. Antibacterial activity of Au/Cur – CNPs

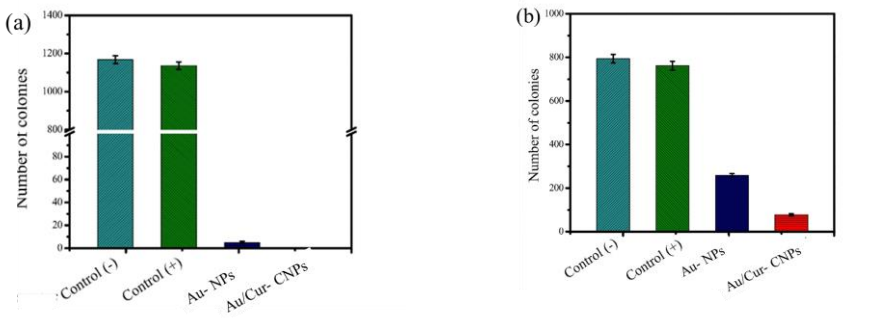

Figure 2.7. (a) Histogram of *MRSA*; (b) Histogram of *E. coli* O157:H7

Comparison between using pure Au - NPs and Au/Cur - CNPs shows that Au/Cur - CNPs significantly enhance the killing and inhibition ability for both Gram-negative and Gram-positive bacterial strains. Under the laser irradiation at the wavelength of 532 nm for 20 min, it was possible to destroy *MRSA* bacteria completely and inhibit the growth of *E.coli* O157:H7 up to 90%.

2.2.6. Evaluation of the cytotoxicity of Au/Cur - CNPs

Toxicity to MA – 104 cells was observed over time when cells were incubated with Au/Cur - CNPs at different concentrations. The monitoring results are listed in the chart Fig. 2.8. Surveying the gradually decreasing concentration, the number of cells that were toxic decreased. After the test from 72h - 144h, the number of living cells remained at 40 - 30%. The number of viable cells at a concentration of 1/16 is over 60%, at concentrations of 1/32 and 1/64, toxic cells are negligible. Thus, the

cytotoxicity of Au/Cur - CNPs is low at the original concentration and safe when the concentration is reduced below 1/16 (< 9.4 ppm).

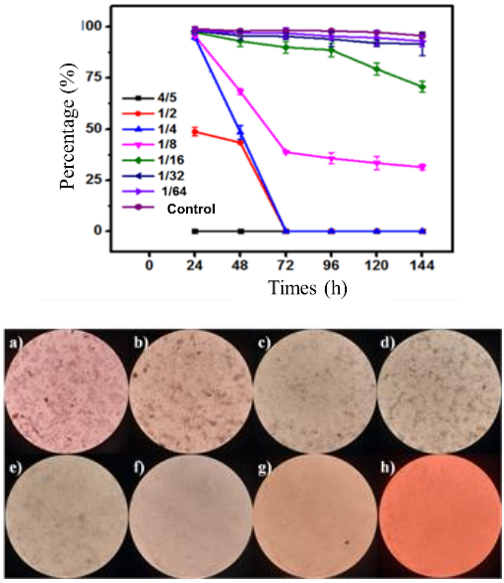

Figure 2.8. Toxicity of Au/Cur - CNPs to MA – 104 cells according to concentration and time. Image of MA104 cells with Au/Cur - CNPs at concentrations a) 4/5, b) 1/2, c) 1/4, d) 1/8, e) 1/16, f) 1/32, g) 1/64 and cell control at 96 hours (200x magnification)

CHAPTER 3. FABRICATION AND CHARACTERISTICS OF GOLD – ZINC OXIDE NANOCOMPOSITES

3.1. Materials and methods

3.1.1. Reagents

Zinc bar (99.99%) size 250 mm x 10 mm x 5 mm and gold (99.99%) bar size 60 mm x 5 mm x 0.1 mm (length x width x height) are purchased at one stop. chemical cave in Hanoi - Vietnam. Sodium citrate ($Na_6H_5O_7$) purchased from Sigma – Aldrich. Other chemicals were of analytical grade.

3.1.2. Experimental method

a. Nanofabrication process of Au/ZnO - CNPs

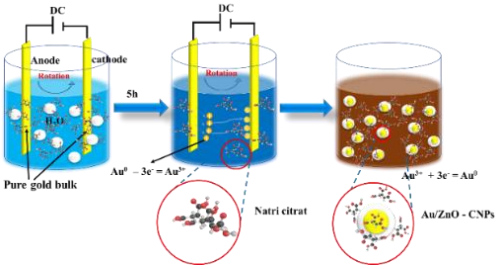

Figure 3.1. Synthesis of Au/ZnO - CNPs by the electrochemical method using two pure gold bars.

b. Characteristics of materials ZnO - NPs and Au/ZnO – CNPs

The particle formation and physicochemical properties of ZnO nanoparticles and Au/ZnO nanocomposites were investigated by UV-vis absorption spectroscopy (SP – 3000 nano, Optima); transmission electron microscope (TEM, JEM1010, JEOL); X-ray diffraction (XRD, EQUINOX 5000, Thermo Scientific). Kinetic size and particle stability in solution Measured DLS kinetic scattering and Zeta potential on the instrument (Zetasizer Nano ZS) and near-IR absorption spectroscopy (FT-IR 4600). The photothermal

measurement system is designed with a blue laser head with a wavelength of 532 nm and a thermal sensor that records temperature over time. Evaluation of antibacterial activity. Evaluation of antibacterial activity based on the photothermal and photocatalytic effects of Au/ZnO - CNPs on the model of 2 bacterial strains causing hospital infections (including *E.coli* O157:H7 and *MRSA*), the ability to MB decomposition ability in the visible region of ZnO - NPs and Au/ZnO – CNPs

3.2. Results and discussion

3.2.1 Optical properties of ZnO - NPs and Au/ZnO - CNPs

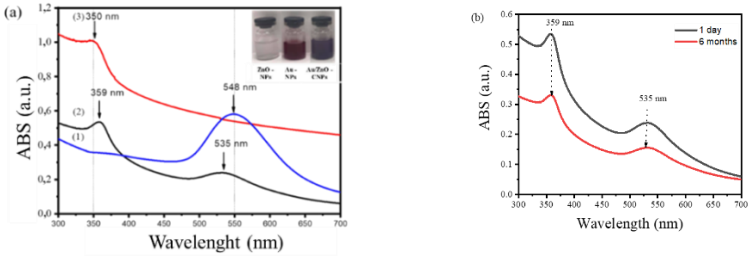

Figure 3.2. UV - Vis absorption spectrum (a) Au – NPs (1), Au/ZnO – CNPs (2) and ZnO - NPs (3) synthesized by the electrochemical method at a voltage of 9V for 5h; (b) Au/ZnO - CNPs synthesized by the electrochemical method at a voltage of 9V for 5 h after storage of 1 day and 6 months.

From the UV-Vis spectrum in Fig. 3.2 (a) it is seen that Au/ZnO – CNPs revealed absorption peaks at a wavelength of 359 nm, typical for ZnO, and 535 nm corresponding to Au. Thus, the appearance of two absorption peaks of ZnO and Au in the solution after electrochemical process and they both shift towards longer wavelengths can mean that Au-ZnO - CNPs have formed in the solution. After 6 months of storage, the absorption peak position of the solution remains unchanged, so the sample is stable for a long period of up to 6 months.

3.2.2 Morphology and structure of ZnO - NPs and Au/ZnO – CNPs

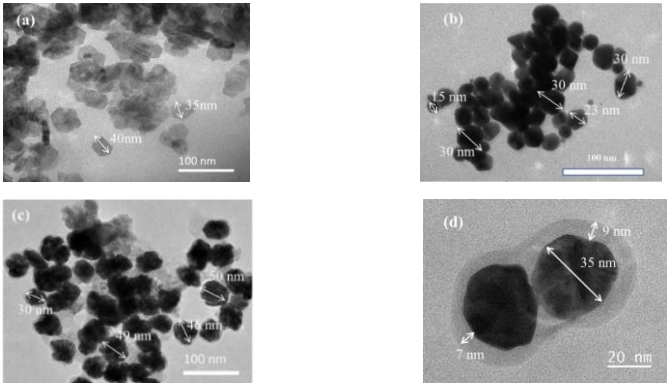

Figure 3.3. TEM image (a) ZnO - NPs; (b) Au - NPs; (c), (d) Au/ZnO - CNPs synthesized by the electrochemical method.

Figure 3.3 (a) shows that the ZnO - NPs have a hexagonal shape, the average particle size is 36.6 nm (Fig. 3.3 a). Fig. 3.3 (b) shows that during the electrochemical process without adding nano ZnO, spherical Au-NPs with uniform sizes ranging from 15 to 30 nm are obtained. Figure 3.3 (c) gold electrochemical product with an added solution containing ZnO - NPs. The gold particles are no longer spherical but instead are heterogeneous Au-NPs with an average particle size of 28.4 nm (Fig. 3.3). When observed with greater magnification in Fig. 3.3(d), the border region of Au-NPs appears as an outer layer with a thickness of 7 nm to 9 nm. Au/ZnO - CNPs have been successfully synthesized with a core of Au - NPs and an outer shell of ZnO - NPs.

X-ray diffraction measurement was performed to further strengthen the argument that the Au/ZnO - CNPs were successfully fabricated by the electrochemical method.

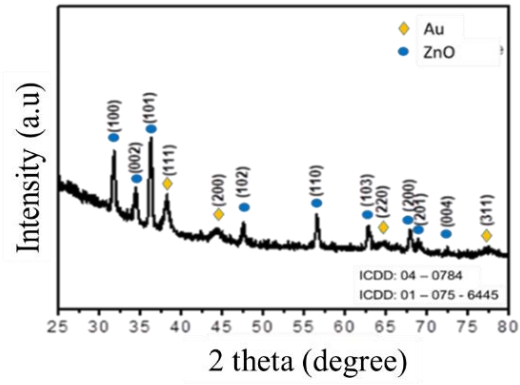

Figure 3.4. X-ray diffraction pattern of Au/ZnO - CNPs synthesized by the electrochemical method at 9V voltage for 5 hours.

The X-ray diffraction pattern shows the appearance of peaks with the Miller index (hkl) (100) corresponding to the angle of $2\theta = 31.77^o$; (002) corresponding to the angle of $2\theta = 34.44^o$; (101) corresponding to the angle of $2\theta = 36.26^o$, and they are characteristic peaks of ZnO - NPs with hecxagonal Wurzite structure (ICDD standard card no 01-075-6445). In addition, four characteristic peaks of the corresponding crystal faces of Au-NPs have a cubic crystal structure according to ICDD standard card no 04 - 0784 with the index *hkl*: (111) at angle $2\theta = 38.27^o$; (200) at angle $2\theta = 44.41^o$; (220) at angle $2\theta = 64.89^o$ and (311) at angle $2\theta = 77.54^o$. The diffraction peaks of both crystal phases are quite sharp, proving that the material obtained after electrochemical crystallization is good. The diffraction peaks of both crystal phases are quite sharp, proving that the material obtained after electrochemical crystallization is good. good does not

exist in an amorphous form. The diffraction pattern shows that in addition to the characteristic peaks of ZnO - NPs and Au - NPs, no diffraction peaks of other phases appear, so the solution only contains Au/ZnO - CNPs without any components. Somewhat different, completely consistent with the UV-Vis measurement results and observed from TEM images.

3.2.3. Antibacterial activity of Au/Cur – CNPs

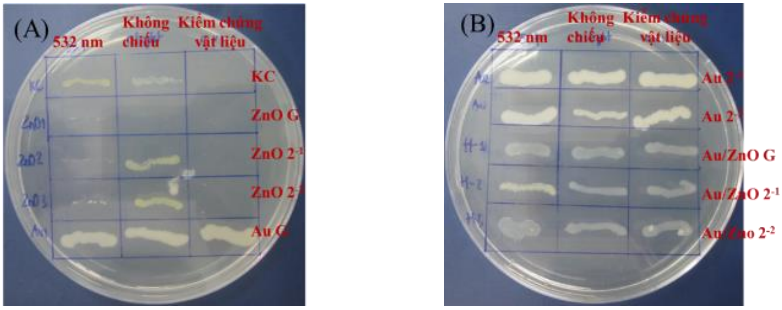

Figure 3.5. Petri dish image: A - nano ZnO - NPs and B- Au/ZnO - CNPs.

The antibacterial ability of ZnO - NPs and Au/ZnO - CNPs was investigated on two strains of Gram-positive (*MRSA*) and Gram-negative bacteria (*E.coli* O157:H7). The gold component in the Au/ZnO - CNPs nanocomposite not only does not have the ability to enhance the antibacterial ability when exposed to light with a wavelength of 532 nm but also negatively affects the antibacterial ability of the ZnO nano - NPs. This can partly be explained by the fact that the temperature increase due to the photothermal effect of Au/ZnO - CNPs is much lower than that of bare Au-NPs.

3.2.4. ***Antibacterial ability of Au/ZnO - CNPs irradiated with the visible light***

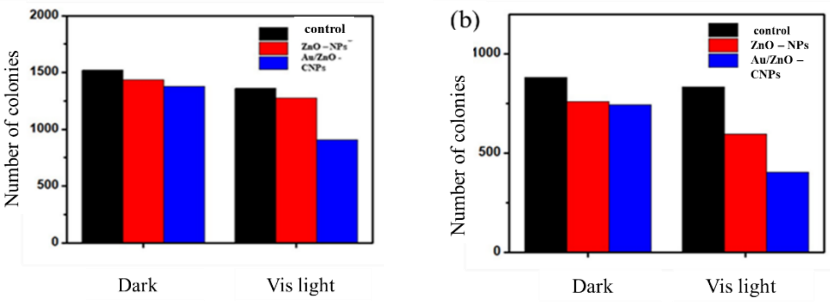

Figure 3.6. Antibacterial activity of Au/ZnO – CNPs with and without visible light irradiation (a) MRSA, (b) *E.coli* O157:H7

Clearly, the antibacterial activity of Au/ZnO - CNPs compared to bare ZnO - NPs on two strains of Gram-positive (MRSA) and Gram-negative bacteria (*E.coli* O157:H7) is enhanced when irradiated with the visible light. The redox radicals ROS formed during incandescent lighting are the main agents that kill pathogen cells. Redox radicals (ROS) can destroy Gram-negative cell membranes more easily than Gram-positive strains. To prove the presence of redox radicals (ROS), the thesis investigated the photocatalytic effect when irradiated with visible light through the decomposition of MB.

3.2.5. *Characteristics of the Au/ZnO - CNPs through investigating the photocatalytic effect*

MB decomposition efficiency increases dramatically in the presence of Au nanoparticles in the Au/ZnO - CNPs. It can be seen that after 30 minutes of adsorption in the dark, only a small amount of MB (about 7%) was adsorbed onto the Au/ZnO - CNPs surface. This is immediately followed by visible light irradiation. The MB concentration decreased rapidly as shown by the degradation reaching more than 30% after 30 minutes of irradiation. After 60 minutes of irradiation, MB decomposition efficiency reached 65% and reached 100% after only 90 minutes of irradiation. This sudden increase in MB

decomposition efficiency of the Au/ZnO - CNPs is explained by the surface plasmon resonance phenomenon of Au - NPs under visible light irradiation.

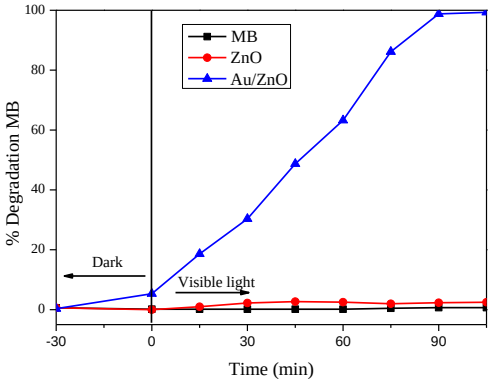

Figure 3.6. Effective photocatalytic degradation of MB of composite materials.

CHAPTER 4. FABRICATION AND CHARACTERISTICS OF GOLD–SILVER NANOCOMPOSITES

4.1. Materials and methods

4.1.1. Reagents

Two silver bars (99.99% purity) with dimensions of 150 mm x 10 mm x 0.5 mm (length x width x thickness), were purchased from a jewellery store in Hanoi, Vietnam and used as two electrodes. Chloroauric acid 99.99% ($HAuCl_4.5H_2O$) and Trisodium citrate ($Na_3C_6H_5O_7$) were purchased from Sigma–Aldrich. All other chemicals used in the project are of analytical grade.

4.1.2 Experimental method

a. Nanofabrication of Au/Ag - CNPs

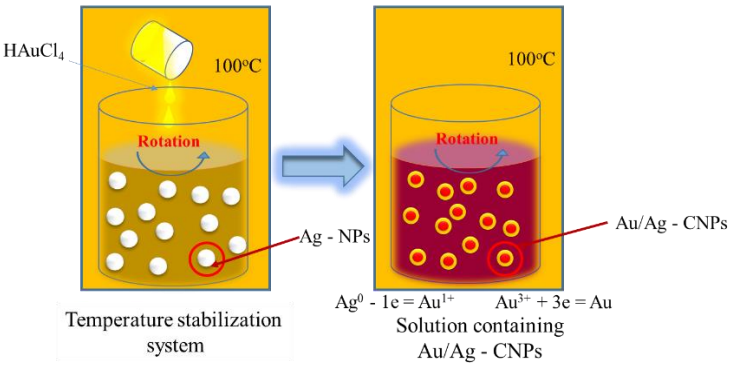

Figure 4.1. Synthesis of Au/Ag - CNPs by the galvanic exchange reaction from clean Au-NPs prepared by the electrochemical method.

b. Characteristics of Au/Ag – CNPs

The formation and physicochemical properties of Au/Ag - CNPs were studied by UV-vis absorption spectroscopy (SP - 3000 nano, Optima), transmission electron microscopy (TEM, JEM1010, JEOL) and X-ray diffraction (XRD, EQUINOX 5000, Thermo). The antibacterial activity of Au/Ag -CNPs was tested on two strains of Gram-positive (*MRSA*) and Gram-negative (*E.coli* O157:H7) bacteria under non-illumination.

4.2. Results and discussion

4.2.1. Optical properties of Au/Ag - CNPs

Fig. 4.2 is the UV-vis absorption spectrum of Ag - NPs with characteristic peaks at the corresponding wavelength of 407 nm. Figure 4.2 also reveals the absorption spectrum of the Ag/Au - CNPs prepared by the electrochemical method. It can be seen that there is an absorption peak at a wavelength of 490 nm, typical for Au - NPs. It is clear that the appearance of the plasmon absorption peak corresponds to Au-NPs and the loss of the

silver absorption peak. Thus, it is clear that Ag-NPs are lost and instead gold nanoparticles appear.

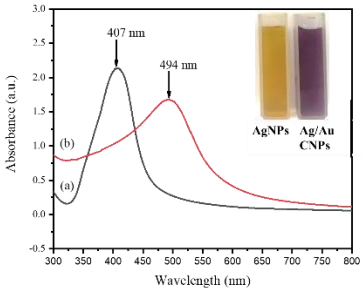

Figure 4.2. UV - Vis absorption spectrum of Au/Ag -CNPs and Ag -NPs; ratio of $HAuCl_4$: Ag - NPs is 1:1.

4.2.2. Morphology and structure of Au/Ag – CNPs

TEM images show that most of Au-NPs are spherical in shape. There are also some rod-shaped Au-NPs. Specifically, observing each particle, the dark and light colors on Au-NPs are not uniform, which proves that Au-NPs have a hollow structure. The particle size ranges from 15 to 30 nm, the average particle size is 23.34 nm.

X-ray diffraction (XRD) pattern of the sample fabricated with Ag: HAuCl4 ratio of 1:1 at a temperature of 100 ^oC (Figure 4.3). The results show that three characteristic diffraction peaks of gold nanorods are observed at $2\theta = 37.38^o$, 43.52^o and 63.94^o corresponding to the crystal facet families (200); (220) and (311), respectively (JCPDS No. 00-004-0784). There is no diffraction peak characteristic of impurities. Thus, it can be said that the silver atom has been electrochemically replaced by a gold atom and has become an ionic state dissolved in solution.

(a) (b)

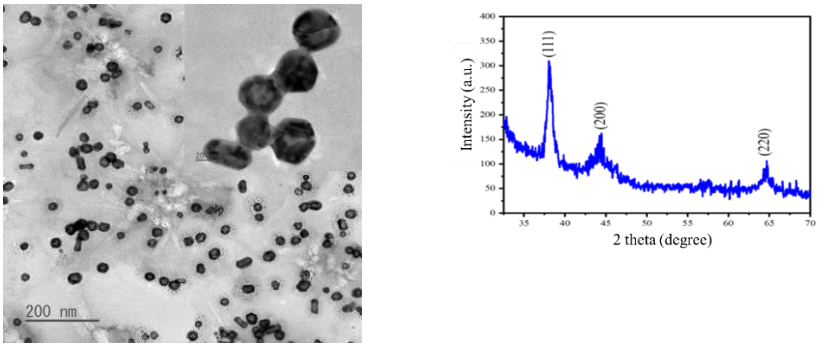

Figure 4.3. TEM image and X-ray diffraction pattern of Au/Ag - CNPs synthesized with Ag: HAuCl4 ratio of 1:1 at a temperature of 100 ^{o}C (A) TEM image; (B) X-ray diffraction pattern.

4.2.3. Antibacterial ability of Au/Ag - CNPs

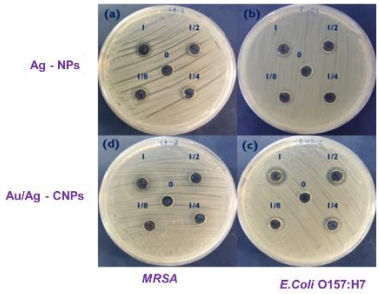

Figure 4.4. The antibacterial activity of Ag - NPs and Ag/Au - CNPs was determined by the disc diffusion technique. Two bacterial strains tested with Ag-NPs against MRSA (a), E. coli O157 :H7 (b); Ag/Au - CNPs against *E. coli* O157:H7 (c) and *MRSA* (d)

The antibacterial activity of Au/Ag-CNPs was tested against two strains of Gram-positive (*MRSA*) and Gram-negative (*E.coli* O157:H7) bacteria. The experimental design and parameters are presented in the experimental section above. At high concentrations, the ability of Au/Ag -

CNPs to inhibit *MRSA* was more effective than that of *E.coli* O157:H7. Au-NPs posed high cytocompatibility and low cytotoxicity. The antibacterial ability of pure Au-NPs was low at room temperature. Thus, it could be concluded that the antibacterial ability of Au/Ag - CNPs was due to the Ag component in the solution. The results showed that the antibacterial ability of Au/Ag - CNPs was enhanced in comparison with that of Ag - NPs.

CONCLUSIONS - RECOMMENDATIONS

CONCLUSIONS

The thesis has been successfully performed to achieve the objectives of the study, there are some main results contributed to the thesis, including:

1. Gold based-nanocomposites of natural compounds (gold-curcumin: Au/Cur – CNPs), inorganic nanosystems (gold - zinc oxide: Au/ZnO – CNPs and gold – silver: Au/Ag – CNPs) have been successfully synthesized. Among them, Au/Cur – CNPs and Au/ZnO – CNPs were synthesized using a simple electrochemical method, which is environmentally friendly with no residues after the reaction. The Au/Cur – CNPs were nearly spherical with an average diameter of 13.6 nm and showed two UV – Vis absorption peaks at 350 nm and 325 nm. In addition, they were stable and well dispersed in water. On the other hand, Au/ZnO - CNPs posed a heterostructure with a gold core layer with an average diameter of 28.4 nm and a ZnO shell with a thickness of 7 – 9 nm, exhibiting 2 UV-Vis absorption peaks at 359 nm and 535 nm. Au/Ag - CNPs were synthesized by the galvanic exchange reaction using silver nanoparticles as templates. Au/Ag – CNPs were nearly spherical with an average diameter of 23.3 nm, showing a UV – Vis absorption peak at 494 nm.

2. Enhanced bacterial inhibiting/killing effects of Au/Cur-CNPs were successfully investigated against representative Gram-negative and Gram-positive bacteria causing hospital-acquired infections via the photothermal effect, in comparison with pure curcumin. The study showed that the antibacterial activity of Au/Cur - CNPs against *MRSA* was enhanced by 20% compared to that of curcumin at the same concentration. After 20 minutes of laser exposure at 532 nm, the photothermal effect of nano gold allowed the release of curcumin molecules to completely kill *MRSA* bacteria and also inhibited the growth of *E.coli* O157:H7 by up to 90%. In addition, the cytotoxicity of the Au/Cur – CNPs was evaluated. The results showed that it was not toxic at concentrations below 9.5 ppm.

3. Enhanced bacterial inhibiting/killing effects of Au/ZnO – CNPs were investigated under the visible light on bacteria causing hospital-acquired infections, in comparison to those of pure ZnO - NPs. The study showed that the antibacterial ability of Au/ZnO - CNPs was unclear despite the light excitation. It might be due to the formation of a ZnO shell which reduced the photothermal effect, leading to a decrease in the bacterial killing effect of Au/ZnO - CNPs. However, under irradiating with visible light, the effects of Au/ZnO – CNP were at 59.5% and 45.6%, higher than those of pure ZnO on both representative Gram-negative and Gram-positive strains, respectively. The antibacterial mechanism of Au/ZnO - CNPs was explained via the photocatalytic effect of those nanosystems under visible light evaluated using methylene blue degradation.

4. Enhanced bacterial inhibiting/killing effects of Au/ZnO – CNPs were investigated without light excitation. The study showed that, at the same

concentration, Ag/Au - CNPs exhibited a better antibacterial effect of 114.3% and 40% compared to silver nanoparticles on Gram-positive bacteria *MRSA* and Gram-negative bacteria *E. coli* O157:H7, respectively. The minimum inhibitory concentration of Au/Ag – CNPs against *MRSA* strain (MIC > 0.83 mM) is lower than that of *E.coli* O157:H7 (MIC > 1.63 mM).

RECOMMENDATIONS

Thanks to our results achieved, we propose the following orientation of ressearch topics:

- Investigating the ability of Au/Cur – CNPs to kill pathogens; Au/ZnO – CNPs; Au/Ag - CNPs based on the photothermal effect under the influence of near infrared radiation;

- Investigating the cytotoxicity/ability to inhibit cancer cell growth of Au/ZnO – CNPs and Au/Ag – CNPs;

- Testing the ability to deliver and release drugs of gold nanoparticles synthesized by the galvanic exchange reaction method.

LIST OF THE PUBLICATIONS RELATED TO THE DISSERATION

ISI publications

1. Nguyen Xuan Quang, Nguyen Thi Luyen, Nguyen Thi Hue, Pham Tuyet Nhung, Nguyen Tien Khi, Nguyen Thanh Thuy, Vu Dinh Lam, Anh – Tuan Le, Nguyen Thi Thu Thuy, Tran Quang Huy, "Formation and antibacterial activity of heterogeneous zinc oxide nanoparticle greenly synthesized by the electrochemical method under microwave treatment" Colloids and Surfaces A: Physicochemical and engineering Aspects, 2023. Volume 674, 5 October 2023, 131906.

Domestic journals and conference publications

2. Xuan-Quang Nguyen, Van-Quang Nguyen, Thu-Thuy Nguyen Thi, Dinh-Lam Vu, Quang-Huy Tran, "The photothermal effect of gold nanoparticles prepared by electrochemical method at different voltages", HPU2.Nat.Sci.Tech,Vol. 2 No. 2, 2023.

3. Nguyễn Xuân Quang, Nguyễn Thị Thu Thủy, Nguyễn Tiến Khí, Trần Quang Huy, "Đặc tính của nano ZnO chế tạo bằng phương pháp điện hóa ở nhiệt độ phòng", Hội nghị Vật lý Chất rắn và Khoa học Vật liệu Toàn quốc – SPMS 2021, trang 850 - 854, năm 2022.

4. Nguyễn Xuân Quang, Vũ Đình Lãm, Trần Quang Huy, "Đặc tính lí hóa của hạt nano vàng lai Au/ZnO chế tạo bằng phương pháp điện hóa" Hội nghị Vật lý Chất rắn và Khoa học Vật liệu Toàn quốc – SPMS 2021, trang 845 – 849, năm 2022.

Useful solution and Patents

5. Patent " Method for producing clean gold nanoparticles with hollow structure for drug delivery", Decision to accept application 111023/QD – SHTT dated November 30, 2023 issued by the Intellectual Property office of Vietnam.

6. Useful solution " Production process of heterogeneous zinc oxide nanomaterials with antibacterial activity", Decision to accept application 111000/QD – SHTT dated November 30, 2023 issued by Intellectual Property office of Vietnam.

7. Patent " Fabrication process of AuNPs/Cur nanomaterials by electrochemical method", Decision to accept application 333564/QD – SHTT dated May 24, 2023 issued by Intellectual Property office of Vietnam.

8. Patent " Thermostatic electrochemical module and production process of gold nanomaterials from gold bars ", Decision to accept application 128065/QD – SHTT dated December 29, 2023 issued by Intellectual Property office of Vietnam.